Master of Science

Functional study of apoptosis inducing protein in human cholangiocarcinoma

The Graduate School

of the University of Ulsan

Department of Medical Science

Hong-Rae Jeong

Functional study of apoptosis inducing protein in human cholangiocarcinoma

Supervisor: Dong-Hoon Jin

A Dissertation

Submitted to

The Graduate School of the University of Ulsan`

In partial Fulfillment of the Requirements

For the Degree of

Master of Science

By

Hong-Rae Jeong

Department of Medical Science

Ulsan, Korea

August 2021

Functional study of apoptosis inducing protein in human cholangiocarcinoma

This certifies that the dissertation of Hong-Rae Jeong is approved

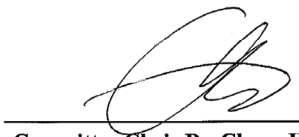

Committee Chair Dr. Chang Hoon Ha

Committee Member Dr. In Ki Kim

Committee Member Dr. Dong-Hoon Jin

Department of Medical Sciences

Ulsan, Korea

August 2021

ABSTRACT

Apoptosis-inducing protein (AIP) is a secreted protein, synthesized by adipocytes and epithelial cells, that is downregulated in breast, colorectal, gastric, liver, and lung cancers, portending a poor prognosis. AIP is a potential biomarker of cancer progression, but its role in cholangiocarcinoma, a cancer of the bile duct, remains unknown. In this study, we found that *AIP* mRNA, but not protein, is expressed in cholangiocarcinoma. However, AIP protein overexpression induced cell death, apoptosis, and sub-G1 arrest. Importantly, AIP-induced apoptotic changes were blocked by knockdown of the pro-apoptotic protein BID, suggesting that AIP-induced apoptosis occurs via BID-dependent pathways. Mechanistically, ELF25 (E3 Ligase Factor25) directly targets AIP by ubiquitination and degradation. Similarly, AIP protein expression was downregulated in cholangiocarcinoma, thus negatively correlating with ELF25 expression in this cancer. Of note, low AIP, combined with high ELF25, expression, correlated with short patient survival in cholangiocarcinoma. Additionally, *ELF25* knockdown led to AIP upregulation, to inhibit growth of cancer cells. Taken together, these results suggest that AIP could be a potential therapeutic target or a diagnostic biomarker, to treat patients with this insidious malignancy.

Keywords: apoptosis-inducing protein, apoptosis, therapeutic target, biomarker, cholangiocarcinoma.

CONTENTS

LIST OF FIGURES

LIST OF TABLES

INTRODUCTION

Cholangiocarcinoma (CCA) is a devastating cancer generating from different locations within the bile ducts, and is classified as extrahepatic and intrahepatic, according to tumor location (Yang et al., 2011). CCA is a fatal cancer with poor overall survival (OS) and late diagnosis (Razumilava & Gores, 2014). Although the associated risk factors for CCAs are cirrhosis, primary sclerosing cholangitis, diabetes, obesity, gallstones, and chronic hepatitis B and C, the main cause of CCA remains unclear (Valle, Lamarca, Goyal, Barriuso, & Zhu, 2017). And in South Korea, the mortality for CCA is high (incidence > 6 per 100,000 habitants), while it is also increasing worldwide (Banales et al., 2020). Since the exact carcinogenic cause of CCA remains undiscovered, there is no appropriate curative treatment except for surgical resection (Andresen et al., 2015; Nakamura et al., 2015; Pant, Peixoto, Richard, & Gradilone, 2020). However, the possibility of surgical treatment depends on the characteristics of the tumor, e.g., the presence of lymph node involvement and distant metastases, tumor differentiation, local extent of the tumor, neural perineal and/or microvascular involvement and lymphatic vessels, etc., the operation is performed for the purpose of radical resection. However, at the time of cancer diagnosis, fewer patients can receive surgical treatment, and the prognosis of surgery is also poor. In addition, CCA is diagnosed through the discovery of a mass-forming lesion through CT, MRI, and biopsy, before surgery. However, CCA is obscured by the liver and stomach, thus confounding its diagnosis via detection or biopsy. Therefore, at the time when symptoms such as weight loss and malaise appear, CCA is already found to have progressed, and most patients die within 1 year, with a dismal 5-year OS rate for stage 3 and 4 CCA of 10% and 0%, respectively (Cillo et al., 2019; Doherty, Nambudiri, & Palmer, 2017; Han et al., 2002). A first-line combination of gemcitabine and cisplatin administration to patients who are not surgical candidates only slightly slows CCA progression, and is not curative (Waseem & Patel, 2017). So, the discovery of new biomarkers, through molecular mechanism research, is crucial to improve the outcome of this fatal disease.

Apoptosis-inducing protein (AIP) is a 40-kDa protein encoded on chromosome 7q22.1, expressed mostly in epithelial cells (Albertus et al., 2008). AIP was first found to relate to lipid denaturalization in cachexia and obesity (Tisdale). AIP downregulates PTEN-Akt signaling, to eventually suppress tumor progression , via repressing the epithelial-to-mesenchymal transition (EMT) by blocking TGFβ1-ERK2 signaling in hepatocellular carcinoma and pancreatic cancer (Kong et al., 2010; Tian et al., 2017; Xu et al., 2016). AIP also prevents soft tissue sarcoma cell migration and invasion (J. Liu et al., 2018). Low AIP expression levels show a poor survival rate in breast cancer, and poor prognosis in primary gastric cancer, while AIP overexpression induces apoptosis and inhibits cell growth, through the mTOR/PTEN signaling pathway, in gastric cancer cells (Huang et al., 2013; Parris et al., 2014). Nevertheless, the role of AIP, in CCA, remains unclear.

Bcl-2 protein family members, major modulators of cell survival and death by regulating apoptosis, are divided into three groups: anti-apoptotic proteins (Bcl-w, Bcl-xL, Bcl-2, and Mcl-1), BH3-only proteins (BAD, BIM, BID, NOXA, PUMA, BMF, BIK, and HRK), and pro-apoptotic effector proteins (BAX, BAK, and BOK). and a balance between the anti– and pro-apoptotic proteins determines apoptosis commitment (Wong, 2011). The mechanisms of apoptosis are classified into two main apoptotic pathways: the death receptor pathway (extrinsic) and the mitochondrial pathway (intrinsic) (Elmore, 2007). When the intrinsic pathway is activated, pore formation occurs, in conjunction with the BH3-only protein BID, during proteolysis of tBID (truncated BID). (Baines & Molkentin, 2009). BID is activated and cleaved by caspase-8 (Billen, Shamas-Din, & Andrews, 2008), facilitating cytochrome C release from the inner mitochondrial membrane, to the cytosol, through a pore (Ott, Robertson, Gogvadze, Zhivotovsky, & Orrenius, 2002). After that, cytochrome C binds to Apaf-1 and procaspase-9, to activate this complex, known as the "apoptosome" (Bao & Shi, 2007). Finally, apoptosome cleaves caspase-3, prior to apoptotic cell death (Dehkordi, Tashakor, O'Connell, & Fearnhead, 2020).

The E3 ligase factor (ELF) protein family generally has a preserved RING domain at the N-terminus, with E3 ubiquitin ligase activity (Hatakeyama, 2011). ELF25 is an ELF family member with E3 ligase activity that mediates proteasomal degradation by ubiquitination of PPARγ, regulation of adipocyte differentiation (Lee et al., 2018), and regulates antiviral signaling, in concert with RNA-binding activity (Choudhury et al., 2017; Gack et al., 2007). ELF25 promotes cell growth and survival in prostate cancer by regulating p53 signals, and in hepatocellular carcinoma, by modulating the antioxidant Keap1-Nrf2 pathway (Y. Liu et al., 2020; Takayama et al., 2018). In addition, ELF25 is an interaction partner with AIP (Lee et al., 2018).

In this study, we confirmed AIP expression levels in CCA cells, and identified its role in apoptotic cell death, in CCA cells. Functional investigation further revealed that AIP is ubiquitinated by ELF25 for proteasomal degradation. We likewise confirmed that apoptotic cell death by AIP, in CCA cells, is mediated by BID apoptosis signaling.

MATERIAL & METHODS

1. Cell culture

Human HEK293 embryonic kidney cells were purchased from ATCC (American Type Culture Collection, Manassas, VA, USA), and cholangiocarcinoma (CCA) cell lines (SNU-308, SNU-478, SNU-1079, SNU-1196) were obtained from KCLB (Korea Cell Line Bank, Seoul, Korea). The cell lines were maintained in RPMI-1640 medium or DMEM (WELGENE, Daegu, Korea) supplemented with 10% fetal bovine serum (GIBCO, Grand Island, NY, USA) and 100 mg/ml penicillin-streptomycin (WELGENE, Daegu, Korea), in a 5% CO_2 incubator, at 37°C.

2. Transfection of plasmids and short hairpin RNAs (shRNAs)

Cells were transiently transfected with target plasmids using Lipofectamine® 2000 reagent (Thermo Fisher Scientific, Waltham, MA, USA), according to the manufacturer's instructions. Wild-type *AIP*, in pCMV sport6, was purchased from the Korea Human Gene Bank (Daejeon, Korea). AIP mutants (AIP K84R, K91R) were mutated into the pCMV sport6 vector. Wild-type human ELF25, and its deletion mutants, were kindly provided by Dr. V. Narry Kim**.** Negative control scrambled shRNAs, with no significant homology to human gene sequences, were used to control for nonspecific effects. The integrity of the constructs was confirmed by sequencing. Targeting the *ELF25*, *BID*, *BIM*, and *PUMA* coding regions, with shRNAs, was used to silence gene expression. Cells were transfected with the target siRNA and shRNA using Lipofectamine® RNAiMAX reagent (Thermo Fisher), according to the manufacturer's instructions. The siRNA and shRNA oligonucleotides were synthesized by Genolution (Seoul, Korea). The sequences of shRNAs against *ELF25*, *BID*, *BIM*, and *PUMA* are listed in Table 1.

3. Analysis of cell death

Cells were collected, suspended in PBS, and diluted two-fold with a trypan blue stain solution (0.4 % (GIBCO)). 10 μL of the mixture was placed on a hemocytometer glass (Marienfeld-Superior, Lauda-Königshofen, Germany), and analyzed using a light microscope (Olympus, Tokyo, Japan) with 10× magnification. Both viable (not stained) and non-viable (stained) cells were counted in the hemocytometer, according to the manufacturer's instructions, and the percentage of dead cells, to the total, was calculated. For each sample, triplicate measurements were conducted.

4. Apoptosis analysis

Cells, incubated under different conditions, were collected, washed with PBS, resuspended in 500 µl 1X binding buffer, and stained with 3 µl annexin V FITC and 5 µl of propidium iodide. Cells were then incubated in the dark at room temperature for 15 minutes, and analyzed by flow cytometry (FACS, BD Biosciences, San Jose, CA).

5. Cell cycle analysis

Cells incubated under different conditions were harvested, washed with PBS, and fixed in 90% methanol overnight at -20 . Cells were then washed with PBS and incubated with propodium iodide (50 µg/ml), in PBS, with RNase (100 µg/ml), in the dark at 4 for 20 min. After incubation, the samples were analyzed by flow cytometry (FACS, BD Biosciences).

6. Immunoblotting and immunoprecipitation

Cells were lysed in RIPA buffer (T&I, Kangwon, Korea), for 30 min on ice, and centrifuged at 4 at 13,000 rpm, for 20 min, to collect supernatants. Protein concentrations were measured by Bradford assay (Bio-Rad, Hercules, CA, USA), samples mixed with loading buffer, and boiled. These samples were electrophoresed by sodium dodecyl sulfate polyacrylamide gel electrophoresis (SDS-PAGE), and transferred to polyvinylidene difluoride (PVDF) membranes for incubation with primary antibodies. Anti-AIP was purchased from Abcam (Cambridge, MA, USA); anti-ELF25 was from BD Biosciences; anti-β-actin was from Santa Cruz Biotechnology (Santa Cruz, CA, USA); and anti-HA-TAG, anti-PARP, anti-cleaved-caspase-3, and anti-cleaved-caspase-9 were from Cell Signaling Technology (Danvers, MA, USA). Then, the membranes were incubated with horseradish peroxidase-conjugated secondary antibodies (Santa Cruz Biotechnology), and protein bands detected using an enhanced chemiluminescence western blotting detection kit (Amersham, Little Chalfont, Buckinghamshire, UK).

For AIP immunoprecipitation, cell lysates were rotated with AIP antibody at 4 , overnight. The beads were then incubated with protein A/G agarose (Thermo Fisher Scientific), at 4 °C for 4 h, washed in RIPA buffer five times, boiled, and analyzed by immunoblotting.

7. Reverse transcription-polymerase chain reaction analysis (RT-PCR)

Total RNA was extracted using TRIzol® (Invitrogen, Carlsbad, CA, USA), and 20 µg of total RNA was used for cDNA synthesis, with random hexamers. *AIP* and *ELF25* mRNA were normalized to

GAPDH mRNA. PCR reactions began with a predenaturation step for 5 min at 95°C; followed by 25 cycles of denaturation at 95°C for 1 min, primer annealing at 58°C for 30 sec, and primer extension at 72°C for 1 min. Primer sequences for *AIP*, *ELF25*, *BID*, and *GAPDH* are listed in Table 2.

8. Ubiquitination assays

HEK293 cells, grown in 10-cm dishes, were co-transfected with / without pSG5-HA-ubiquitin, HA-ELF, wild type AIP, and mutant AIP. 24 h after transfection, the cells were treated with 20 μM MG132 (proteosome inhibitor), for 3 h, and harvested. Cell pellets were resuspended in RIPA buffer (0.1% SDS, 1% Nonidet P-40, 1% EDTA, 50 mm Tris-HCl pH 8.0, 150 mm NaCl, 2 mm EDTA, complete Mini-Protease mixture (1 tablet/50 ml, Roche Applied Science)). 500 μg of the cell lysates was incubated with anti-AIP. After this step, the precipitated pellets were washed 3X with buffer (0.5 % Nonidet P-40, 20 mm Tris-HCl pH 8.0, 120 mm NaCl, 1 mm EDTA), resuspended in 2 × SDS sample buffer, resolved by 6% SDS-PAGE, and analyzed by Western blot using an anti-HA antibody.

9. Statistical analysis

All the results are presented as means ± standard deviations, and each test was repeated at least three times. All statistical analyses were performed with GraphPad Prism (San Diego, CA, USA) software, using two-way analysis of variance (ANOVA), followed by t-tests, to determine significance.

RESULTS

1. AIP protein is downregulated in human cholangiocarcinoma cells

To examine the correlation between AIP expression, with clinical relevance to cholangiocarcionma, we compared AIP levels in normal and cancerous tissues using the and Gepia databases. According to Gepia, Low expression of AIP mRNA was correlated with poor overall survival of the cholangiocarcinoma patients, compared to normal, tissues (Figure 1A). By accessing TCGA data through the UALCAN database, AIP mRNA levels were found to be underexpressed in CCA types (Figure 1B), and similar results were also found in CCA cell lines, at the mRNA (Figure 1C) and protein (Figure 1D) levels.

2. AIP induces apoptotic cell death in human cholangiocarcinoma cells

To determine a possible role for AIP in cholangiocarcinoma cell death, we transfected its coding sequence into SNU-1079 and SNU-478 cells for 72 h and compared these to control cells (Figure 2A). This showed that AIP overexpression activated cleavage of PARP, caspase-9 (cleaved-caspase-9), and caspase-3 (cleaved-caspase-3), in SNU-1079 and SNU-478 cells (Figure 2B), indicating stimulation of a pro-apoptotic signal (late apoptosis), in addition to AIP-overexpressing SNU-1079 and SNU-478 cells demonstrating annexin-V/PI staining (early apoptosis, Figure 2C-D). In addition, an increase in sub-G1 cell debris was observed with PI staining of ectopic AIP-expressing cells (Figure 2E-F). Taken together, these results show that AIP overexpression, in cholangiocarcinoma cells, activates apoptosis.

3. BID mediates apoptosis, via AIP, in human cholangiocarcinoma cells

To investigate the role of AIP in apoptosis signaling, we knocked down BH-3 only proteins (facilitators of mitochondrial apoptosis), under AIP overexpression conditions, finding that only BID knockdown strongly abolished AIP-induced apoptosis in SNU-1079 cells (Figure 3A). In addition, BID knockdown reduced cleavage of caspase-3 (cleaved caspase 3) (Figure 3 B-C), also confirming remarkably decreased apoptosis in AIP-overexpressing SNU-1079, compared to control, cells, by annexin-V/PI staining (Figure 2D-E) Taken together, these results show that AIP induces apoptosis in cholangiocarcinoma cells via BID signaling.

4. AIP and ELF25 protein expression reversely correlate

To assess why AIP is lowly expressed in cholangiocarcinoma cells, we examined both AIP and ELF25 expression levels. According to Gepia, high expression of ELF25 mRNA was correlated with poor overall survival of the cholangiocarcinoma patients, compared to normal, tissues(Figure 4A), By accessing TCGA data through the UALCAN database, AIP and ELF25 mRNA levels were found to negatively correlate in cholangiocarcinoma types (Figure 4B), which also affirmed protein levels by western blot data (Figure 4C-D)

5. ELF25 influences AIP protein levels, and apoptosis, in cholangiocarcinoma cells

To assess how ELF25 affects AIP in cholangiocarcinoma cells, co-immunoprecipitation (co-IP) was conducted to confirm ELF25 as a binding partner of AIP (Figure 5A). Next, we used a series of truncated mutants of ELF25, and constructed an AIP mutant with Lys 84 or Lys 91 changed into Arg (Figure 5B). Co-immunoprecipitation further demonstrated that only the ELF25 ΔN mutant (containing the PRY/SPRY domain) interacted with AIP (Figure 5C). As a ubiquitin E3 ligase, ELF25 presumably binds to, and mediates the ubiquitination of AIP, causing AIP degradation. Moreover, immunoprecipitation assays demonstrated decreased ubiquitination of AIP mutants (Figure 5D). Taken together, these results showed that the ELF25 binds AIP to mediate its ubiquitination, and subsequent proteasomal degradation.

6. ELF25 directly ubiquitinates AIP to promote its degradation

To further determine ELF25 effects on AIP apoptotic activity, we established knocked down TRM25 in cholangiocarcinoma cells, and selected shELF25 #1 for further investigation (Figure 6A). While ELF25 knockdown had no effect on AIP mRNA levels (Figure 6B), it did induce AIP protein levels, in SNU-1079 cell (Figure 6C). To examine the effects of ELF25 on cholangiocarcinoma cell death, we knocked it down, resulting in induction of apoptotic cell death, compared to control cells, as shown by annexin-V/PI staining (Figure 6D-E). Taken together, these results show that ELF25 affects AIP protein levels, and apoptosis, in cholangiocarcinoma cells.

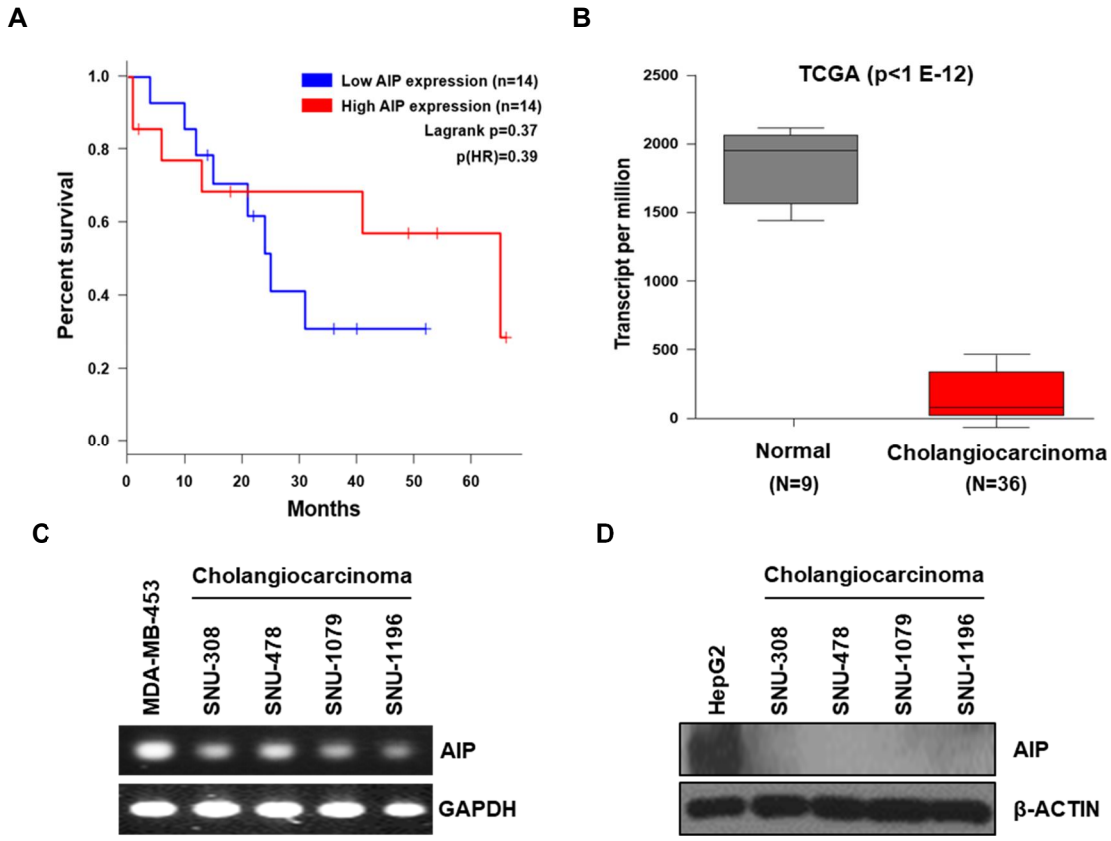

Figure 1. AIP expression in cholangiocarcinoma. (A) The Gepia database showed a Kaplan-Meier curve for AIP high and low expression group of cholangiocarcinoma (indicate Logrank p=0.37, p(HR)=0.39, compared to normal). (B) The UALCAN database further indicated AIP expression in TCGA cholangiocarcinoma samples (indicate p<1E-12 compared to normal). (C) mRNA expression levels of AIP and GAPDH in four human cholangiocarcinoma cells. MDA-MB-453 breast cancer cells, positive control (D) Western blot analysis of AIP and β-actin levels in four human cholangiocarcinoma cells. HepG2 hepatocellular cancer cells, positive control.

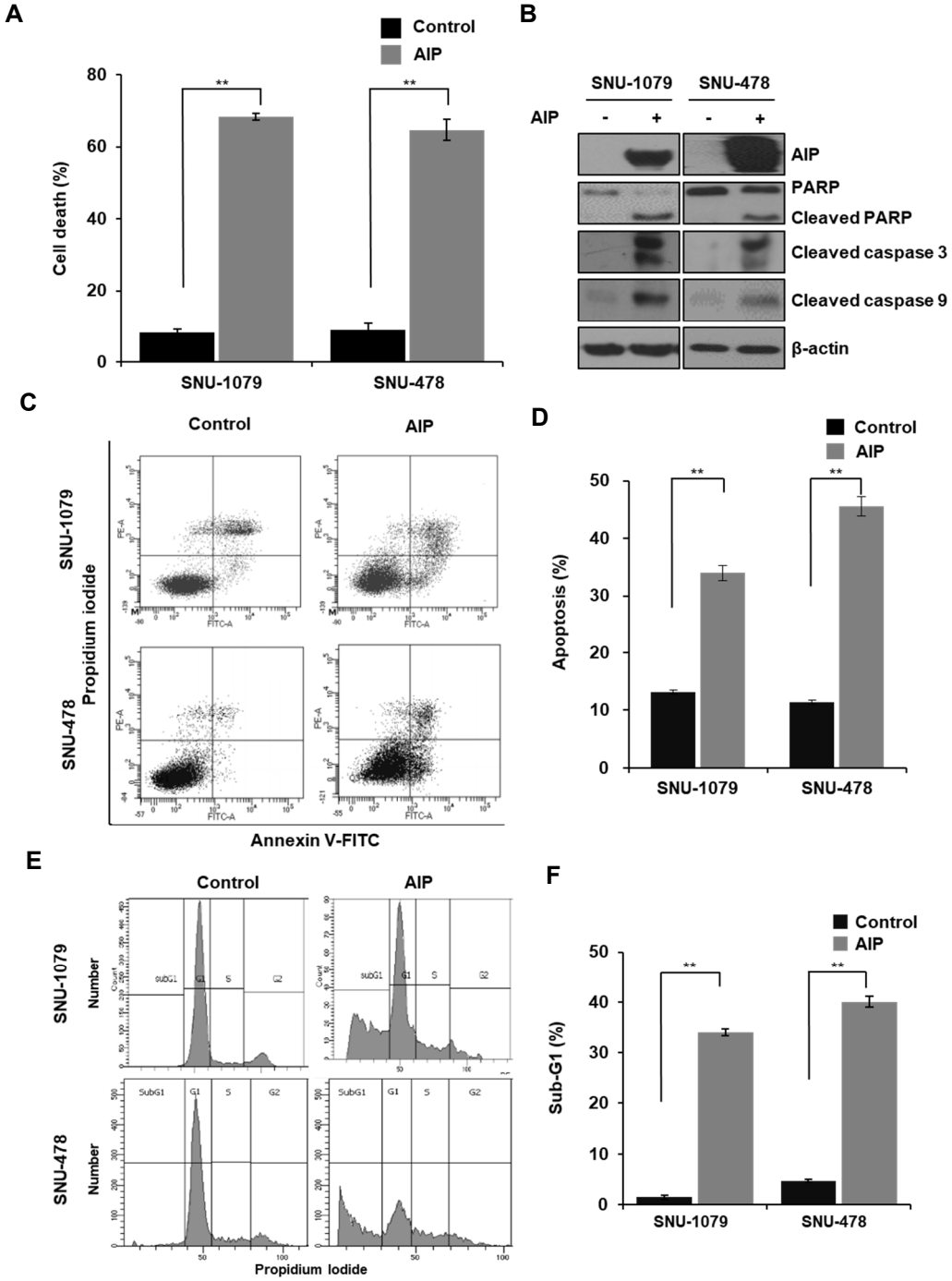

Figure 2. AIP-induced apoptosis in cholangiocarcinoma cells. (A) SNU-1079 and SNU-478 cells were transfected with AIP for 72 h, and cell death determined by hemocytometry (B) Western blot analysis of AIP, cleaved-PARP, cleaved-caspase-3, cleaved caspase-9, and β-actin in SNU-1079 and SNU-478 cells overexpressing control or AIP for 24 h. (C) Apoptosis analysis by annexin-V/PI staining and cytometry, with quanitification of three independent flow cytometry experiments by bar charts (D) (E) Cell cycle analysis was performed using PI staining and flow cytometry, as quantified by bar charts (F) All flow cytometry experiments were performed 72 h after overexpressing AIP in cholangiocarcinoma cells. **, $p<0.005$ indicates significant differences from the control group.

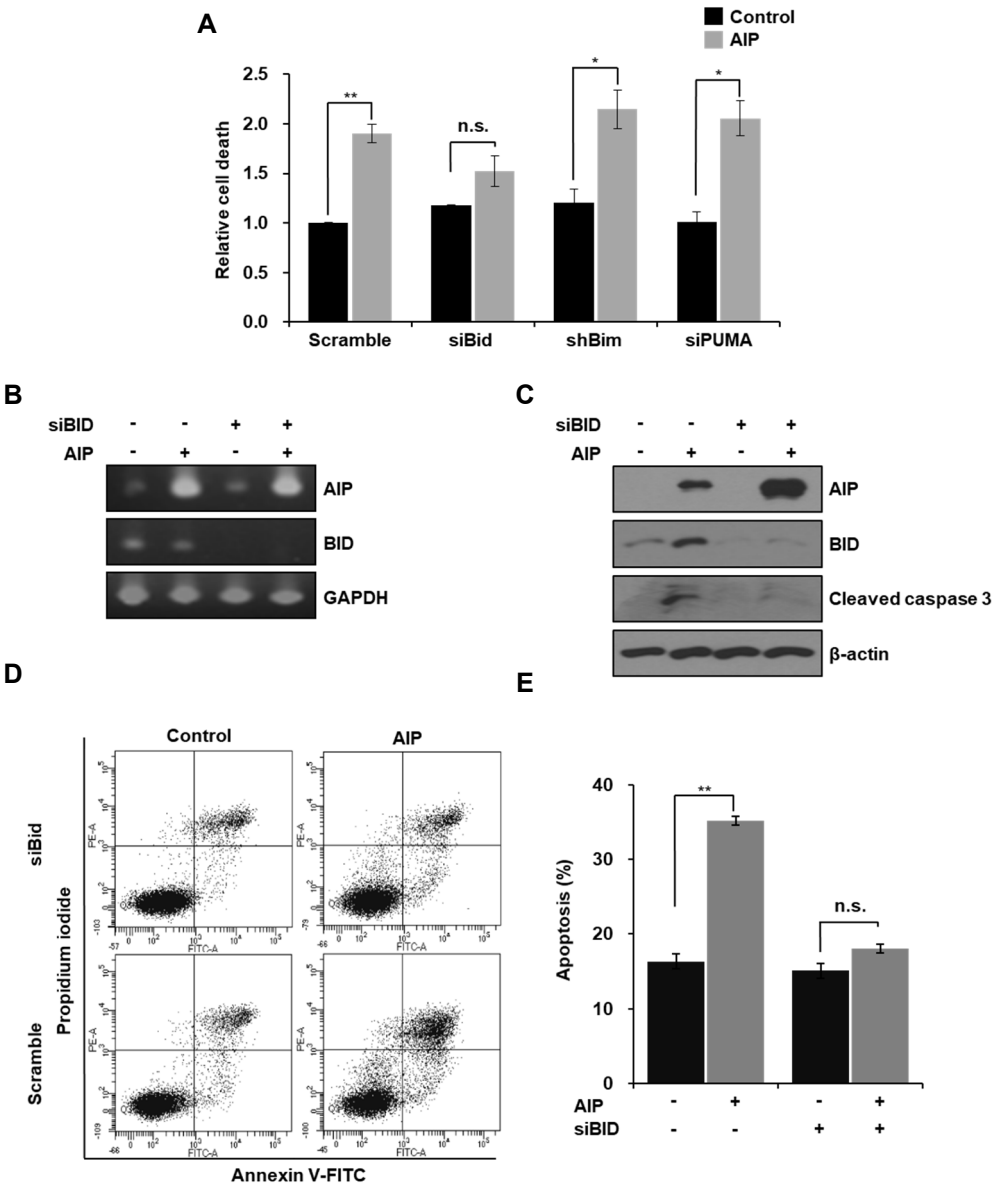

Figure 3. AIP induces BID-dependent apoptosis in SNU-1079 cells. (A) Relative cell death after AIP overexpression and/or knockdown of pro-apoptotic proteins. Overexpressed AIP after 24 h knockdown of pro-apoptotic proteins, and cell death determination by hemocytometry, after overexpressing control or AIP, for 72 h. (B)-(E) All experiments were performed after overexpressing control or AIP for 72 h, including (B) mRNA expression levels of AIP, BID, and GAPDH; (C) Western blot analysis of levels of AIP, BID, β-actin, and cleaved-caspase-3; (D) Apoptotic cell death analysis, by annexin-V/PI staining and flow cytometry. (E) Bar charts show quantitative data of the average of three independent flow cytometry experiments. *, $p<0.05$ and **, $p<0.005$ indicate significant differences from the control group.

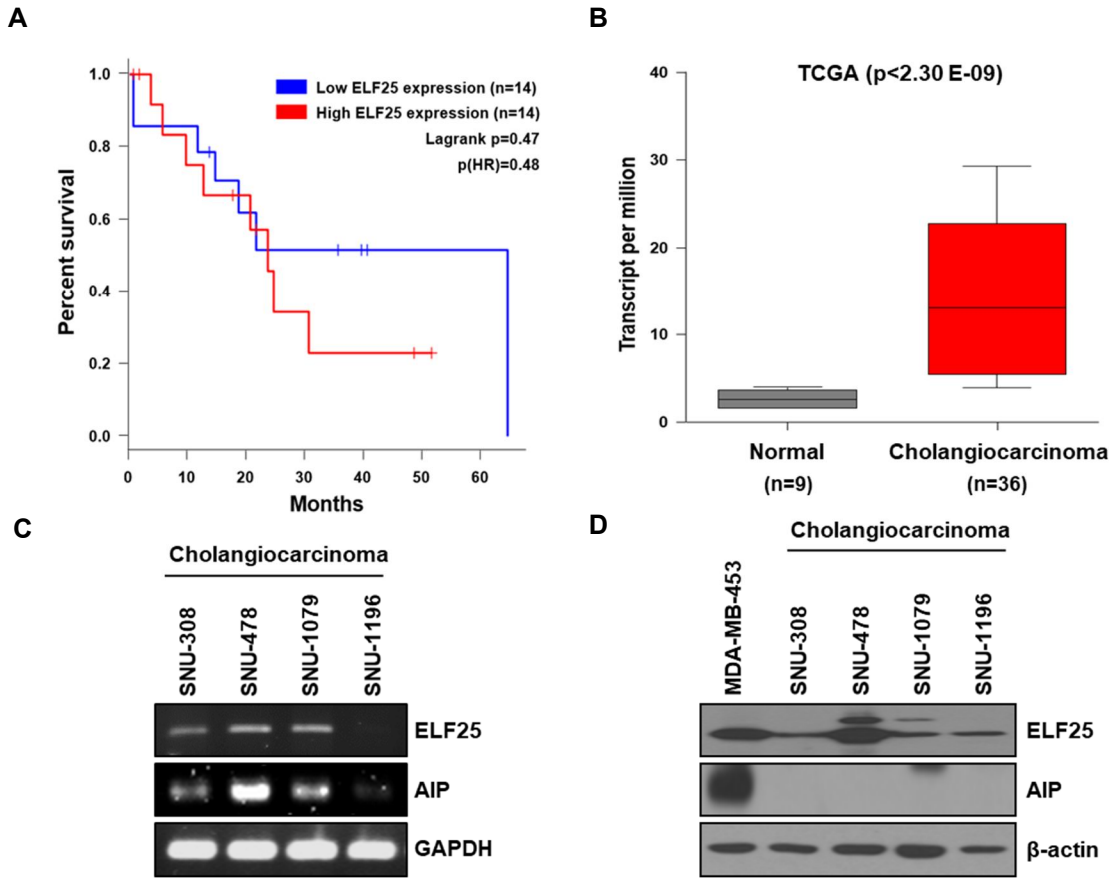

Figure 4. AIP and ELF25 expression reversely correlate. (A) The Gepia database showed a Kaplan-Meier curve for ELF25 high and low expression group of cholangiocarcinoma (indicate Logrank p=0.47, p(HR)=0.48, compared to normal). (B) ELF25 expression (indicate p=2.29E-09 compared to normal). (C) mRNA expression levels of ELF25, AIP, and GAPDH, in four human cholangiocarcinoma cells. (D) Western blot analysis of the levels of ELF25, AIP, and β-actin in four human cholangiocarcinoma cells. MDA-MB-453 breast cancer cells were used as a positive control.

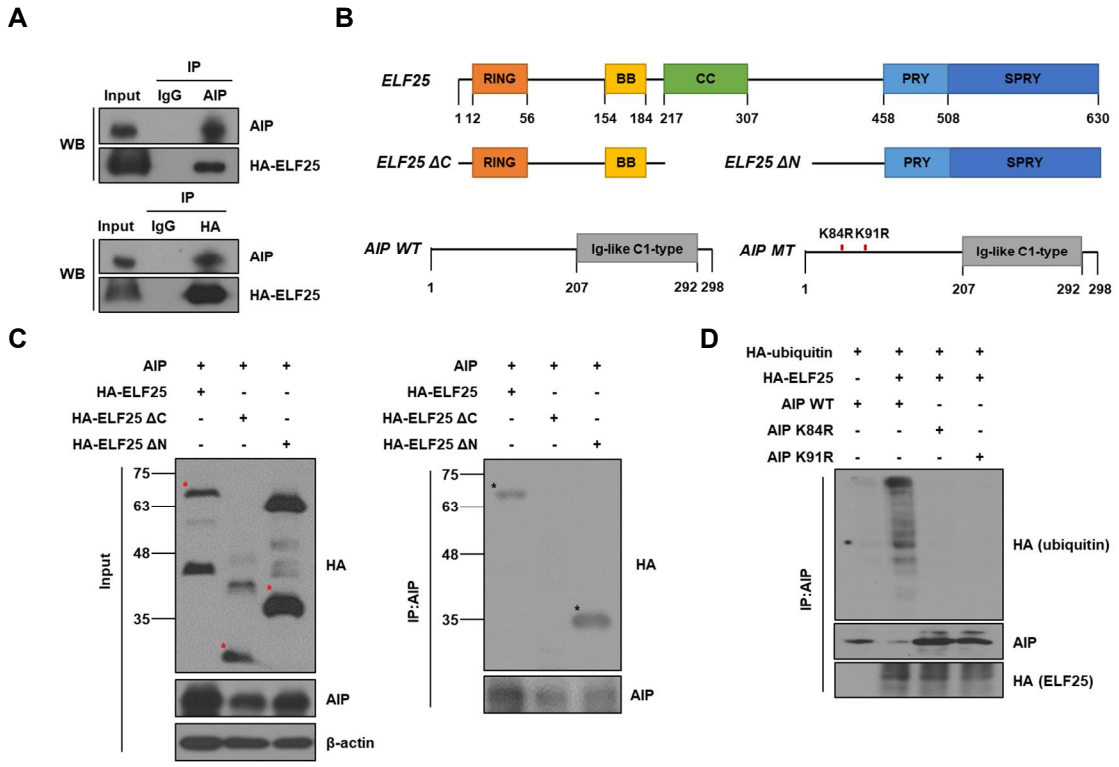

Figure 5. ELF25, an E3 ligase, causes degradation of AIP by binding via its ELF25 PRY/SPRY domain. (A) Coimmunoprecipitation assay of interaction between AIP and ELF25. (B) Structure of *ELF25*, *ELF25 ΔC*, *ELF25 Δ N*, *AIP wild type*, and its mutant (*AIP K84R* or *K91R*, i.e., the conserved Lys84 and Lys 91 mutated to Arg). (C) HEK293 cells were transfected with *AIP* with *ELF25* WT or *ELF25* mutants. Western blots analysis of AIP and ELF25 after AIP immunoprecipitation. (D) HEK293 cells were transfected with the indicated plasmids. Western blot analysis of ubiquitinated wild type and mutated AIP, using the indicated antibodies.

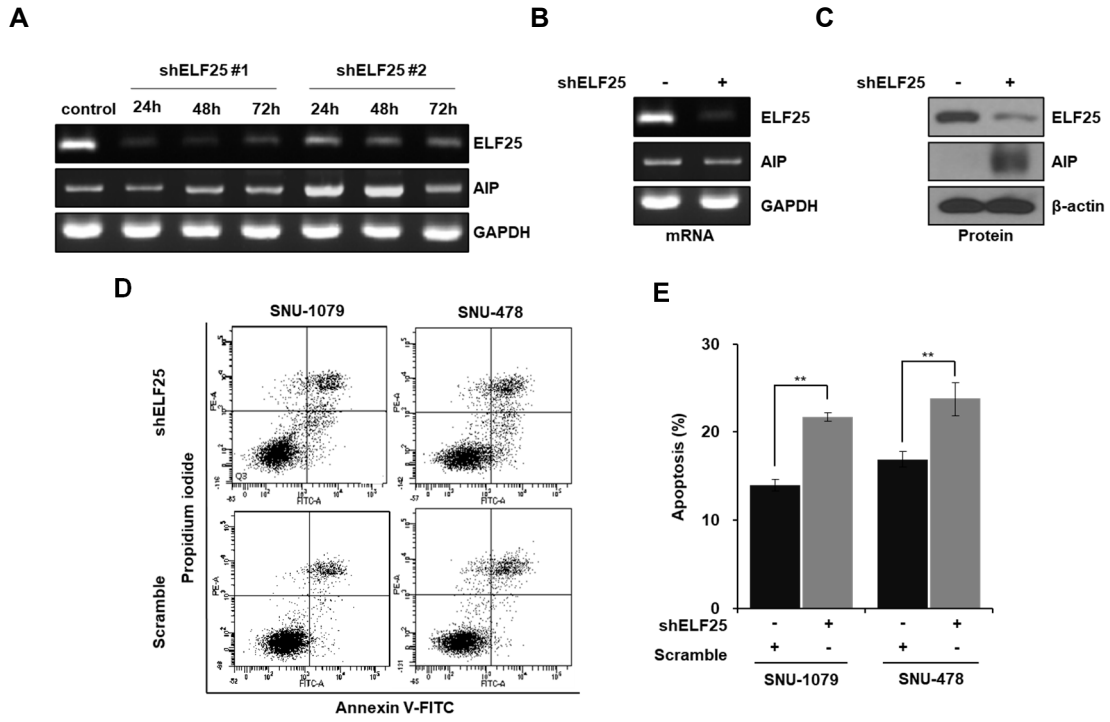

Figure 6. ELF25 regulation of AIP stability affects apoptosis. (A) mRNA expression levels of ELF25, AIP, and GAPDH after 24h, 48h, and 72h *ELF25* knockdown, in SNU-1079 (B) mRNA expression levels of ELF25, AIP, and GAPDH (C) Western blot analysis of ELF25, AIP, and β-actin levels 24h after knockdown of *ELF25*, in SNU-1079 cells. (C) Apoptotic cell death analysis was performed after 24h *ELF25* knockdown in cholangiocarcinoma cells, using annexin-V/PI staining and flow cytometry. (D) Bar charts show quantitative data of the average of three independent flow cytometry experiments. *, $p<0.01$ and **, $p<0.005$ indicate significant differences from the control group.

Table 1. siRNA and shRNA sequences list.

Gene name	Sequences (5' – 3')
shELF25	#1 GGUGGAGCAGCUACAACAA UCUC UUGUUGUAGCUGCUCCACC UU
	#2 GGAAAAGAAAUCCAAGAAA UCUC UUUCUUGGAUUUCUUUUCC UU
shBIM	GACCGAGAAGGUAGACAAUUG UCUC CAAUUGUCUACCUUCUCGGUC UU
siBID	Sense-AAGAAGACAUCAUCCGGAAUAUU
	Antisense- UAUUCCGGAUGAUGUCUUCUUUU
siPUMA	Sense-ACGAGCGGCGGAGACAAGAGGAGCAUU
	Antisense- UGCUCCUCUUGUCUCCGCCGCUCGUUU

Table 2. Primer sequences list.

Gene	Primer sequences (5' – 3')	
AIP	Sense	CAG AAG CAG CGG AGC ATT CT
	Anti-sense	TGC CTC CCA CTT CTG CTT GG
BID	Sense	TGA GGT CAA CAA CGG TTC CA
	Anti-sense	GGA AGC CAA ACA CCA GTA GGT T
ELF25	Sense	CAG ACC TTG AAG GAG GAG ATT G
	Anti-sense	GAG AGC AGT ATG TGA ACC TCT G
GAPDH	Sense	GGA CTG AGG CTC CCA CCT TT
	Anti-sense	CCT GCA GCG TAC TCC CCA CA

DISCUSSION

Cholangiocarcinoma, a cancer of the bile duct, is difficult to diagnose, due to its locational characteristics in the liver and upper part of the liver. Resultantly, the cancer is typically detected in its 3rd and 4th stages, largely negating possible curative surgical treatment. In addition, even after surgical removal, recurrence is high, with an average 5-year survival rate of 10% (Khan & Dageforde, 2019; Rizvi & Gores, 2013). In the case of stage 3 or 4 cholangiocarcinoma patients who cannot be treated surgically, a combination therapy of gemcitabine and cisplatin is currently being used, although the prognosis is poor, and the median overall survival is less than 1 year (Rizvi, Khan, Hallemeier, Kelley, & Gores, 2018). Recently, pemigatinib, a small molecule that inhibits fused or rearranged fibroblast growth factor 2 (FGFR2), has been approved by the FDA as a targeted treatment for CCA. However, the corresponding patients' survival was as low as 10% in the total CCA, and the response rate was also reported in the 30% range (Hoy, 2020). Therefore, potential therapeutic targets and the CCA diagnosis marker are still needed. AIP is involved in fat degeneration and lipid degradation of cachexia and adipose tissue, and when overexpressed in carcinoma cells, it acts as a tumor suppressor by inhibiting migration and invasion and reducing proliferation. In addition, the possibility of AIP as a biomarker in several carcinomas has been suggested (Huang et al., 2013; J. Liu et al., 2018; Parris et al., 2014; Tian et al., 2017; Yu, Ling, Yu, Du, & Liu, 2020).

In this study, we set forth to overcome the limitations of existing CCA treatment by studying AIP as a new treatment target or diagnostic biomarker in CCA, discovering AIP as a tumor suppressor in CCA. In silico data showed that *AIP* RNA expression level was high in CCA, while its protein expression was lower in normal tissues. And the same result was confirmed at the level of RNA and protein in CCA cells. To assess its role in CCA cells, we overexpressed AIP, demonstrating induction of apoptotic cell death. To further investigate CCA cell apoptosis by AIP, we examined the involvement of specific Bcl2 families. So, we used a single siRNA or shRNA sequence, for knockdown of each Bcl2 family member in AIP-overexpressing CCA cells, and measured cell death. As a result, when BID was inhibited, we confirmed that CCA cell apoptosis by AIP decreased, compared to control cells, demonstrating BID mediation of CCA cell apoptosis by AIP. To provide insight into reasons why AIP was expressed highly, at the RNA level, but low at the protein level, we investigated physical interaction between AIP and ELF25 in CCA cells, based on ELF25 having E3 ligase activity involved in adipocyte differentiation, and promoting cancer cell growth (Lee et al., 2018). As a result, we found that ELF25 interacts with AIP to ligate ubiquitin. In addition, we confirmed that AIP protein upregulation, and apoptotic cell death, increased after *ELF25* knockdown. Altogether, this shows that AIP induces apoptotic cell death through the activation of BID in CCA, which is inhibited by ELF25.

Although we herein investigated the role of AIP in CCA for the first time, an AIP signaling pathway mechanism in CCA should be confirmed. For example, TGFβ signaling pathway is a main pathway that promotes CCA progression. Many studies report that the TGFβ induces EMT in CCA cells (Papoutsoglou, Louis, & Coulouarn, 2019), while TGFβ signaling (and carcinogenesis) is blocked by AIP. Consequently, loss of AIP leads to EMT, accompanied by the promotion of invasion, reduced apoptosis and proliferation, pro-survival signals, and a shift in energy metabolism (Kong et al., 2010; Xu et al., 2016). Additionally, there are no reports of an AIP signaling pathway in CCA. Further studies of AIP signaling pathway in CCA should be conducted, to better clarify its role.

CONCLUSION

In this work, we investigated the role of AIP in CCA, showing that AIP is lowly expressed in CCA, compared to normal bile duct tissue. In AIP-overexpressing cells, we confirmed that AIP induces apoptotic cell death in CCA, which is mediated by BID. Additionally, low AIP expression levels in CCA correlate with high expression level of ELF25, an E3 ligase. By ELF25 knockdown, ELF25 interaction with AIP and ubiquitination decreased, and AIP expression levels increased to induce apoptotic cell death in CCA cells. These findings would suggest the potential of new treatment targets or diagnostic biomarkers in CCA.

REFERENCES

Albertus, D. L., C. W. Seder, G. Chen, X. Wang, W. Hartojo, L. Lin, A. Silvers, D. G. Thomas, T. J. Giordano and A. C. Chang (2008). "AZGP1 autoantibody predicts survival and histone deacetylase inhibitors increase expression in lung adenocarcinoma." Journal of thoracic oncology 3(11): 1236-1244.

Andresen, K., K. M. Boberg, H. M. Vedeld, H. Honne, P. Jebsen, M. Hektoen, C. A. Wadsworth, O. P. Clausen, K. E. Lundin and V. Paulsen (2015). "Four DNA methylation biomarkers in biliary brush samples accurately identify the presence of cholangiocarcinoma." Hepatology 61(5): 1651-1659.

Baines, C. P. and J. D. Molkentin (2009). "Adenine nucleotide translocase-1 induces cardiomyocyte death through upregulation of the pro-apoptotic protein Bax." Journal of molecular and cellular cardiology 46(6): 969-977.

Banales, J. M., J. J. Marin, A. Lamarca, P. M. Rodrigues, S. A. Khan, L. R. Roberts, V. Cardinale, G. Carpino, J. B. Andersen and C. Braconi (2020). "Cholangiocarcinoma 2020: the next horizon in mechanisms and management." Nature Reviews Gastroenterology & Hepatology 17(9): 557-588.

Bao, Q. and Y. Shi (2007). "Apoptosome: a platform for the activation of initiator caspases." Cell Death & Differentiation 14(1): 56-65.

Billen, L., A. Shamas-Din and D. Andrews (2008). "Bid: a Bax-like BH3 protein." Oncogene 27(1): S93-S104.

Choudhury, N. R., G. Heikel, M. Trubitsyna, P. Kubik, J. S. Nowak, S. Webb, S. Granneman, C. Spanos, J. Rappsilber and A. Castello (2017). "RNA-binding activity of TRIM25 is mediated by its PRY/SPRY domain and is required for ubiquitination." BMC biology 15(1): 1-20.

Cillo, U., C. Fondevila, M. Donadon, E. Gringeri, F. Mocchegiani, H. J. Schlitt, J. N. Ijzermans, M. Vivarelli, K. Zieniewicz and S. W. Olde Damink (2019). "Surgery for cholangiocarcinoma." Liver International 39: 143-155.

Dehkordi, M. H., A. Tashakor, E. O'Connell and H. O. Fearnhead (2020). "Apoptosome-dependent myotube formation involves activation of caspase-3 in differentiating myoblasts." Cell death & disease 11(5): 1-12.

Doherty, B., V. E. Nambudiri and W. C. Palmer (2017). "Update on the diagnosis and treatment of cholangiocarcinoma." Current gastroenterology reports 19(1): 2.

Elmore, S. (2007). "Apoptosis: a review of programmed cell death." Toxicologic pathology 35(4): 495-516.

Gack, M. U., Y. C. Shin, C.-H. Joo, T. Urano, C. Liang, L. Sun, O. Takeuchi, S. Akira, Z. Chen and S. Inoue (2007). "TRIM25 RING-finger E3 ubiquitin ligase is essential for RIG-I-mediated antiviral activity." Nature 446(7138): 916-920.

Han, J. K., B. I. Choi, A. Y. Kim, S. K. An, J. W. Lee, T. K. Kim and S.-W. Kim (2002). "Cholangiocarcinoma: pictorial essay of CT and cholangiographic findings." Radiographics 22(1): 173-187.

Hatakeyama, S. (2011). "TRIM proteins and cancer." Nature reviews cancer 11(11): 792-804.

Hoy, S. M. (2020). "Pemigatinib: first approval." Drugs 80: 923-929.

Huang, C.-y., J.-j. Zhao, L. Lv, Y.-b. Chen, Y.-f. Li, S.-s. Jiang, W. Wang, K. Pan, Y. Zheng and B.-w. Zhao (2013). "Decreased expression of AZGP1 is associated with poor prognosis in primary gastric cancer." PloS one 8(7): e69155.

Khan, A. S. and L. A. Dageforde (2019). "Cholangiocarcinoma." Surgical Clinics 99(2): 315-335.

Kong, B., C. Michalski, X. Hong, N. Valkovskaya, S. Rieder, I. Abiatari, S. Streit, M. Erkan, I. Esposito and H. Friess (2010). "AZGP1 is a tumor suppressor in pancreatic cancer inducing mesenchymal-to-epithelial transdifferentiation by inhibiting TGF-β-mediated ERK signaling." Oncogene 29(37): 5146-5158.

Lee, J. M., S. S. Choi, Y. H. Lee, K. W. Khim, S. Yoon, B.-g. Kim, D. Nam, P.-G. Suh, K. Myung and J. H. Choi (2018). "The E3 ubiquitin ligase TRIM25 regulates adipocyte differentiation via proteasome-mediated degradation of PPARγ." Experimental & molecular medicine 50(10): 1-11.

Liu, J., H. Han, Z. Fan, M. El Beaino, Z. Fang, S. Li and J. Ji (2018). "AZGP1 inhibits soft tissue sarcoma cells invasion and migration." BMC cancer 18(1): 1-8.

Liu, Y., S. Tao, L. Liao, Y. Li, H. Li, Z. Li, L. Lin, X. Wan, X. Yang and L. Chen (2020). "TRIM25 promotes the cell survival and growth of hepatocellular carcinoma through targeting Keap1-Nrf2 pathway." Nature communications 11(1): 1-13.

Nakamura, H., Y. Arai, Y. Totoki, T. Shirota, A. Elzawahry, M. Kato, N. Hama, F. Hosoda, T. Urushidate and S. Ohashi (2015). "Genomic spectra of biliary tract cancer." Nature genetics 47(9): 1003-1010.

Ott, M., J. D. Robertson, V. Gogvadze, B. Zhivotovsky and S. Orrenius (2002). "Cytochrome c release from mitochondria proceeds by a two-step process." Proceedings of the National Academy of Sciences 99(3): 1259-1263.

Pant, K., E. Peixoto, S. Richard and S. A. Gradilone (2020). "Role of Histone Deacetylases in Carcinogenesis: Potential Role in Cholangiocarcinoma." Cells 9(3): 780.

Papoutsoglou, P., C. Louis and C. Coulouarn (2019). "Transforming Growth Factor-Beta (TGFβ) Signaling Pathway in Cholangiocarcinoma." Cells 8(9): 960.

Parris, T. Z., A. Kovács, L. Aziz, S. Hajizadeh, S. Nemes, M. Semaan, E. Forssell Aronsson, P. Karlsson and K. Helou (2014). "Additive effect of the AZGP1, PIP, S100A8 and UBE2C molecular biomarkers improves outcome prediction in breast carcinoma." International journal of cancer 134(7): 1617-1629.

Razumilava, N. and G. J. Gores (2014). "Cholangiocarcinoma." The Lancet 383(9935): 2168-2179.

Rizvi, S. and G. J. Gores (2013). "Pathogenesis, diagnosis, and management of cholangiocarcinoma." Gastroenterology 145(6): 1215-1229.

Rizvi, S., S. A. Khan, C. L. Hallemeier, R. K. Kelley and G. J. Gores (2018). "Cholangiocarcinoma—evolving concepts and therapeutic strategies." Nature reviews Clinical oncology 15(2): 95.

Takayama, K.-i., T. Suzuki, T. Tanaka, T. Fujimura, S. Takahashi, T. Urano, K. Ikeda and S. Inoue (2018). "TRIM25 enhances cell growth and cell survival by modulating p53 signals via interaction with G3BP2 in prostate cancer." Oncogene 37(16): 2165-2180.

Tian, H., C. Ge, F. Zhao, M. Zhu, L. Zhang, Q. Huo, H. Li, T. Chen, H. Xie and Y. Cui (2017). "Downregulation of AZGP1 by Ikaros and histone deacetylase promotes tumor progression through the PTEN/Akt and CD44s pathways in hepatocellular carcinoma." Carcinogenesis 38(2): 207-217.

Tisdale, M. J. "Zinc-a2-glycoprotein in cachexia and obesity." Curr Opin Support Palliat Care 3: 000-000.

Valle, J. W., A. Lamarca, L. Goyal, J. Barriuso and A. X. Zhu (2017). "New horizons for precision medicine in biliary tract cancers." Cancer discovery 7(9): 943-962.

Waseem, D. and T. Patel (2017). "Intrahepatic, perihilar and distal cholangiocarcinoma: management and outcomes." Annals of hepatology 16(1): 133-139.

Wong, R. S. (2011). "Apoptosis in cancer: from pathogenesis to treatment." Journal of Experimental & Clinical Cancer Research 30(1): 1-14.

Xu, M.-Y., R. Chen, J.-X. Yu, T. Liu, Y. Qu and L.-G. Lu (2016). "AZGP1 suppresses epithelial-to-mesenchymal transition and hepatic carcinogenesis by blocking TGFβ1-ERK2 pathways." Cancer letters 374(2): 241-249.

Yang, H., T. W. Li, J. Peng, X. Tang, K. S. Ko, M. Xia and M. A. Aller (2011). "A mouse model of cholestasis-associated cholangiocarcinoma and transcription factors involved in progression." Gastroenterology 141(1): 378-388. e374.

Yu, W., J. Ling, H. Yu, J. Du and T. Liu (2020). "AZGP1 suppresses the process of colorectal cancer after upregulating FASN expression via mTOR signal pathway." General Physiology and Biophysics 39(3): 239-248.

국문 요약

담도암은 국내에서 높은 발생 빈도를 보이는 암종으로 5년 생존율이 20-30% 정도로 예후가 좋지 않다. 담도암의 가장 확실한 치료방법은 수술적 절제술이지만, 전산화 단층촬영 (CT)을 통한 발견이 어려워 조기 진단이 거의 이루어지지 않아 담도암에서의 새로운 치료 전략의 수립이 필요하다.

AIP는 상피세포에 많이 발현되어 있으며, cachexia에서 비만 및 지방 변성과 관련된 것으로 처음 보고되었다. 또한, 여러 암에서 항암효과를 보인다는 연구가 보고되고 있으나, 담도암에서의 연구는 현재까지 보고되지 않았다. 인 실리코(*In silico*) 분석에 의하면 담도암에서 AIP의 mRNA는 정상조직에 비해 높게 발현되지만, 단백질은 낮은 발현수준을 보였고, 본 연구에서 이와 동일한 결과를 담도암 세포주에서 확인하였다. 담도암 세포에서 AIP를 과발현 하였을 때, AIP는 세포 자멸사(apoptosis)와 sub-G1 arrest를 유도하였다. 특히, AIP에 의한 세포 자멸사는 세포 자살 촉진 단백질인 BID 저해시에 억제되었다. 따라서, AIP는 담도암에서 BID 의존적인 경로로 세포 자멸사를 유도하는 것을 확인하였다. 한편, 본 연구에서 AIP와 상호작용하며 E3 연결활성을 가진 ELF25가 AIP의 유비퀴틴화를 매개하여 분해를 촉진하는 것을 보였고, 더 나아가 인 실리코 분석으로 AIP와 ELF25의 단백질 발현이 담도암에서 역 상관관계를 가지며 동일한 결과를 담도암 세포주에서 확인하였다. 또한, 낮은 AIP, 높은 ELF25 발현을 보이는 담도암 환자가 더 짧은 생존을 갖는 경향이 있음을 발견하였다. 추가적으로, 담도암 세포에서 ELF25를 억제하였을 때, AIP의 단백질 발현이 증가하고 세포 성장이 저해되는 것을 확인하였다.

본 연구를 통해, 담도암에서 AIP의 기능 및 AIP의 분해 분자기전을 밝혔고, 이러한 AIP의 기능은 담도암 세포의 세포 자멸사를 유도하는 결과를 보여주어 암억제자로써의 역할을 제시하였다. 본 연구결과를 통해 AIP가 담도암 환자에서 잠재적인 치료 표적으로써의 가능성을 제시하였다.

중심 단어: 담도암, AIP, 세포자멸사, 치료 표적, 바이오마커